

A robust and coarse surface mesh modified by interpenetrating polymer network hydrogel for oil-water separation

Jinlong Zhu, Huili Li, Juan Du, Wenchen Ren, Pingping Guo, Shimei Xu, Jide Wang

Key Laboratory of Oil and Gas Fine Chemicals, Ministry of Education and Xinjiang Uyghur Autonomous Region, College of Chemistry and Chemical Engineering, Xinjiang University, Urumqi, Xinjiang 830046, People's Republic of China

Correspondence to: S. Xu (E-mail: xushmei@gmail.com)

ABSTRACT: A robust and coarse surface mesh was fabricated by introducing a hydrogel coating with interpenetrating polymer network (IPN) structure on stainless steel mesh. The IPN hydrogel was prepared by crosslinking polymerization of acrylic acid (AA) followed by condensation reaction of polyvinyl alcohol (PVA) and glutaraldehyde (GA) at room temperature. As a result, the roughness of modified mesh was enhanced obviously and oil droplet underwater showed a larger contact angle. The hydrogel-coated surface showed an underwater superoleophobicity with an oil contact angle of $153.92 \pm 1.08^\circ$. Besides, stable wettability was observed. The mesh can selectively separate oil from water with a high separation efficiency of above 99.8%. This work provides a facile method to strengthen the coating and enhance the efficiency of oil-water separation. © 2015 Wiley Periodicals, Inc. *J. Appl. Polym. Sci.* **2015**, *132*, 41949.

KEYWORDS: coatings; hydrophilic polymers; separation techniques; surfaces and interfaces

Received 9 October 2014; accepted 4 January 2015

DOI: 10.1002/app.41949

INTRODUCTION

Oil-water separation is of great significance in regulation of pollution. The environmental and economic demands emphasize the need for materials that can effectively separate oil and water. It is an effective and facile way to use special wettability to design novel materials like hydrophobic-oleophilic^{1–3} or hydrophilic-oleophobic materials,^{4–8} since oil-water separation is an interfacial challenge. But the hydrophobic-oleophilic materials usually face a challenge that the oil always blocks the material and their working lives are cut down largely,⁹ while the hydrophilic-oleophobic one has good performance in anti-fouling of oil.¹⁰ Especially the latter can be made by constructing the micro-nano bioinspired surface structure.^{11–13}

Recently, a new concept of taking advantage of high-energy materials with water-favoring property to construct underwater superoleophobic surfaces in oil/water/solid three-phase systems is proposed.¹⁴ The underwater superoleophobicity arises from the combination of hierarchical micro-nano structures and the hydrophilic chemistry on the surface.¹⁵ Inspired by the strategy, superoleophobic surfaces in aqueous media have been realized in recent years. Xue et al reported the fabrication of a novel superhydrophilic and underwater superoleophobic mesh by dip-coating the stainless steel mesh with the pre-gel solution of polyacrylamide.¹⁶ It can selectively and effectively separate water from free oil-water mixtures. Other researchers also reported

superhydrophilic meshes for oil-water separation, and the coating varied from polymers¹⁷ to inorganic materials.^{18,19} The latter were reported to had excellent separation efficiency, and the oil content of filtrate varied from several to several dozens ppm.^{18,19} However, in comparison, the polymer coating is more flexible and easy to be functionalized.

Hydrogels are typically hydrophilic polymer networks. Because of their excellent water-absorbing and water-retaining capacities, hydrogels are considered to be promising candidates for designing novel oil-water separation materials.²⁰ Compared with the inorganic modified mesh, the main disadvantage of hydrogel-coated mesh is weak mechanical strength of the hydrogels after swollen.²¹ The hydrogels with interpenetrating polymer network (IPN) structure have been reported to be mechanically strong.²² In our previous work, we successfully prepared tough polyacrylic acid/polyethylene glycol (PAA/PEG) IPN hydrogel, in which the PEG network was crosslinked by glutaraldehyde (GA) via condensation reaction while the PAA network crosslinked by *N,N*-dimethylethylacrylamide (BIS) via free-radical polymerization. The final hydrogel exhibited compressive strength of 10.9 MPa in a water content of 90 wt % due to lightly crosslinking and special entangled bundles morphology. Here we attempt to prepare a robust and coarse surface mesh by introducing IPN structure into PAA/ polyvinyl alcohol (PVA) hydrogel-coating for oil-water separation. PVA was chosen as the linear polymer for its good property of being film and the characteristic of easy

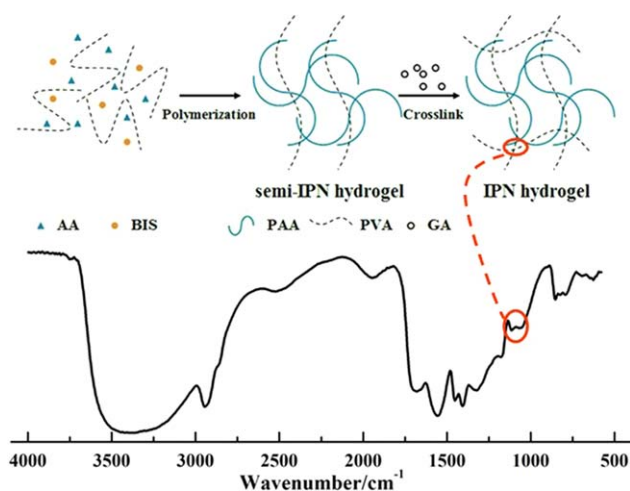


Figure 1. Schematic preparation (above) and FTIR spectrum (bottom) of the IPN hydrogel coating. [Color figure can be viewed in the online issue, which is available at wileyonlinelibrary.com.]

crosslinking.²³ In our experiment, stainless steel mesh was modified to achieve underwater superoleophobicity by free-radical crosslinking polymerization of acrylic acid (AA) in the presence of PVA. Subsequently PVA was crosslinked by GA to form the second polymer network, which interpenetrated into the first PAA network. It was expected that the crosslinking reaction of PVA would cause the first network shrink and produce a coarse surface of coating. The IPN hydrogel-coated mesh showed good wettability and high oil-water separation efficiency.

EXPERIMENTAL

Materials

AA, PVA with a degree of polymerization of 1750 ± 50 and BIS were purchased from Tianjin Guangfu Chemistry Reagent Factory, China; ammonium persulfate (APS) and NaOH were

purchased from Tianjin Chemistry Reagent Factory; N,N,N',N' -tetramethylethylenediamine (TEMED) was purchased from Aldrich Chemical; 25 wt % GA solution (biological reagent) was purchased from China National Medicine Corporation. All reagents were used as received without further purification. The stainless steel mesh was purchased from Jinyuan Screen Company. The deionized water was used in all experiments.

Instrument

FTIR spectra of the dry IPN hydrogel coating was recorded on a BRUKER EQINOX55 spectrometer in a range of $400\text{--}4000\text{ cm}^{-1}$. SEM images of the air-dried and freeze-dried IPN hydrogel-coated mesh were obtained using an electron microscope (LEO-1430VP, LEO, Germany) respectively. Prior to the SEM morphology investigation of the freeze-dried hydrogel, the hydrogel coating was swollen in water to reach equilibrium, and then freeze-dried and sprayed with gold. Contact angles were measured on a JJ2000 B2 machine (POWEREACH, China) at ambient temperature. The oil droplets (1, 2-dichloroethane dyed with methyl red, about $4\ \mu\text{L}$) were dropped onto the prepared mesh under water. The average values of three measurements performed at different positions on the same sample was adopted as the contact angle. Mechanical strength of the hydrogel coating was evaluated by measurement of bulk hydrogels with a tensile-compressive tester (H5KT, Tinius Oisen, USA). The bulk hydrogels were cut into a cube of side length about 1 cm. The abrasion resistance of the hydrogel coating was evaluated by observing the hydrogel loss on the surface. The coated meshes were put into the silica dispersion with a silica size of 300–400 mesh, and then stirring for 4 h before observation by optical microscope (JNOEC XS-212-201). Before the stirring, the coated meshes were immersed in deionized water overnight to reach swelling equilibrium. To test the separation efficiency of both IPN hydrogel coated mesh and semi-IPN one, the oil-water free mixture (oil to mixture is 30 v/v%) was poured straightly to the mesh which was settled between two glass tubes. The oil

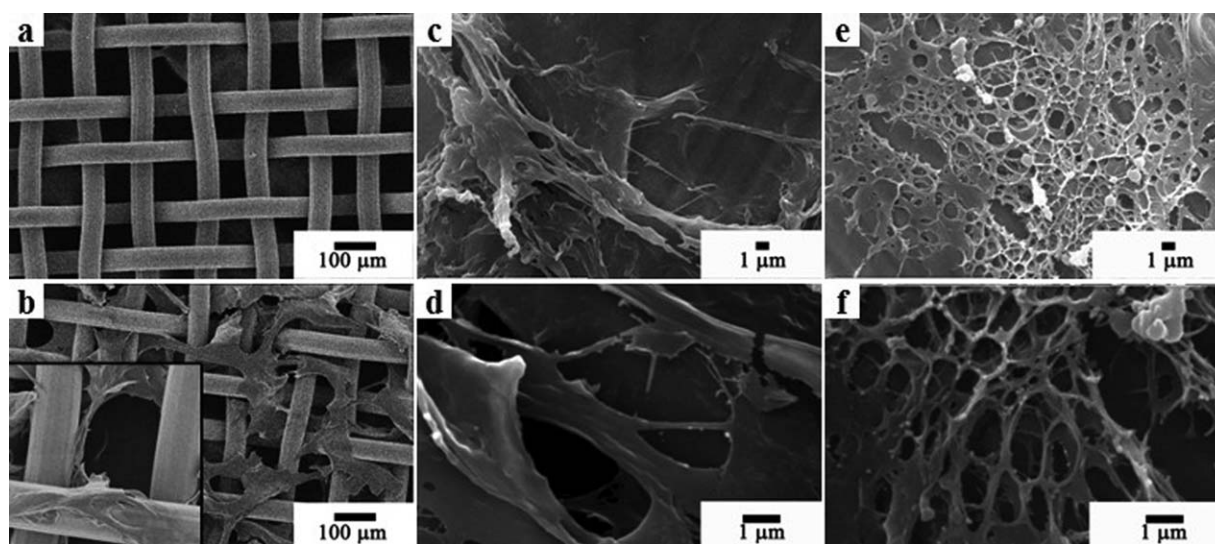


Figure 2. SEM images of the samples (a, stainless steel mesh; b, air-dried IPN hydrogel coating on the mesh; c, d, freeze-dried semi-IPN hydrogel coating on the mesh; e, f, freeze-dried IPN hydrogel coating on the mesh).

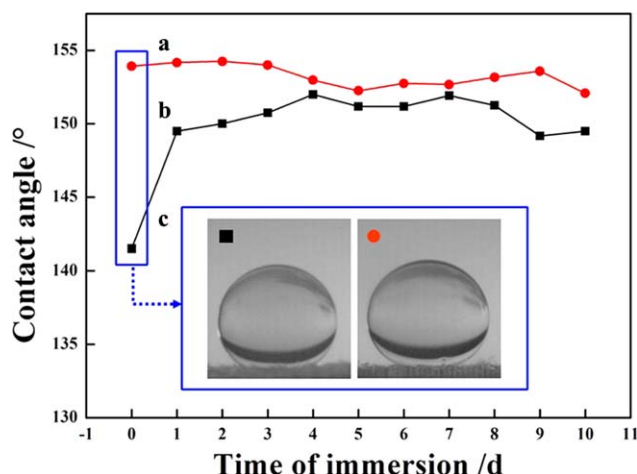


Figure 3. Dependence of immersion time on wettability of the hydrogel coated mesh (a, IPN; b, semi-IPN; c, the graphs of contact angle test for two kinds of hydrogels coated meshes right after immersion). [Color figure can be viewed in the online issue, which is available at wileyonlinelibrary.com.]

content of the collected water after separation was measured by the infrared spectrometer. CCl_4 was used to extract oils from water. The absorbance at 2930 cm^{-1} , 2960 cm^{-1} , and 3030 cm^{-1} were measured. Through calculation with the absorbance and the correction coefficient, the oil content was obtained.

Preparation of IPN Hydrogel-Coated Mesh

AA was added into 4 wt % of PVA solution, and then the neutralization degree of AA was adjusted to 75% with 30 wt % of NaOH solution in an ice water bath for easier polymerization and better hydrophilic ability. Then 2 wt % BIS, 10 wt % of APS and TEMED were added to obtain a pre-gel solution respectively. The ratio of PVA, AA, NaOH, BIS, APS and TEMED is 20:100:42:3:1:0.9 by weight respectively. The clean stainless steel mesh was carefully immersed in the mixed pre-gel solution, and then drawn out horizontally and stand at ambient temperatures over night. Afterwards, the mesh was sprayed with

5 wt % GA solution to obtain a loading amount of 12.6 mg/cm^2 . After crosslinking for 0.5 h, the mesh was washed with abundant deionized water to remove excess GA and unreacted monomers. Finally the mesh was dried at room temperature. As control, the semi-IPN PAA/PVA hydrogel-coated mesh was prepared following the procedure above except that no GA was added.

RESULTS AND DISCUSSION

FTIR Spectra of Coatings

In our experiment, the stainless steel mesh was immersed into the mix pre-gel solution composed of PVA, AA, BIS, APS, and TEMED. Crosslinking polymerization of AA was initiated by APS and TEMED and formed semi-IPN hydrogel. Subsequent crosslinking of GA with PVA via condensation reaction produced the PVA network, which interpenetrated into the PAA network resulting in the formation of IPN PAA/PVA hydrogel (Figure 1 above). In the spectrum of the IPN hydrogel, the stretching of $\text{C}=\text{O}$ in COO^- and COOH of PAA network can be found at 1553 cm^{-1} and 1677 cm^{-1} , respectively. The absorption at 1110 cm^{-1} was ascribed to the stretching of $\text{C}-\text{O}-\text{C}$ groups, which confirmed the successful crosslinking reaction between GA and PVA (Figure 1 bottom). The IR spectra proved the formation of IPN structure.

SEM Morphology

Compared with stainless steel mesh with an average wire diameter of $52.8 \pm 2.2\text{ }\mu\text{m}$ (200 mesh size) [Figure 2(a)], the mesh became rough after coating with the IPN PAA/PVA hydrogel with an average wire diameter of $56.0 \pm 3.0\text{ }\mu\text{m}$ [Figure 2(b)]. Moreover, the hydrogel network was interwoven with the stainless steel mesh forming a coarse surface. To observe the role of GA on the coating morphology, a comparative SEM analysis was made between freeze-dried semi-IPN and IPN PAA/PVA hydrogels [Figure 2(c–f), respectively]. After crosslinking reaction between PVA and GA, the IPN hydrogel coating took an obvious change on morphology. A coarser surface was observed, which might be deduced by more pores and smaller pore size compared with the semi-IPN hydrogel coating.

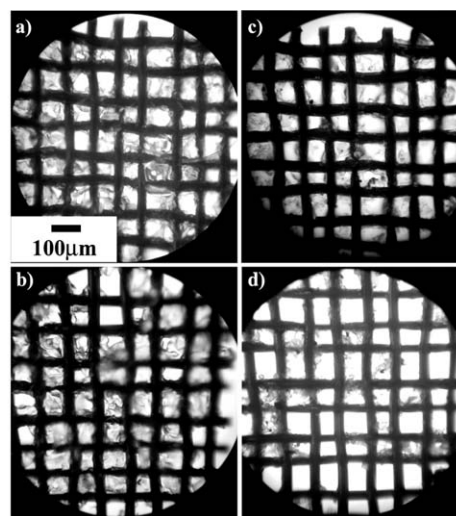
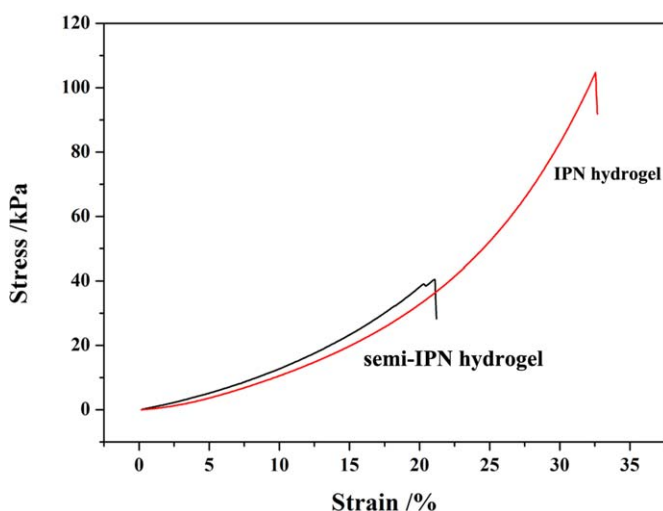
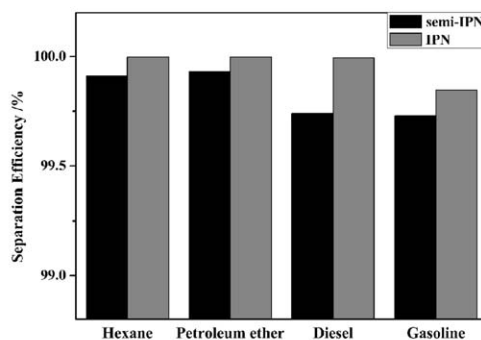


Figure 4. Stress–strain curves for bulk hydrogels under compression (left) and the photographs of hydrogel coated meshes before (a, IPN; b, semi-IPN) and after abrasion resistance test (c, IPN; d, semi-IPN). [Color figure can be viewed in the online issue, which is available at wileyonlinelibrary.com.]



Figure 5. The separation of the hydrogel-coated mesh for oil-water mixtures, and the separation efficiency for each mixture (black is semi-IPN; gray is IPN). [Color figure can be viewed in the online issue, which is available at wileyonlinelibrary.com.]



Mesh Wettability and Mechanical Property

The contact angle of the hydrogel-coated mesh was measured to evaluate the wettability. Figure 3 showed the shape of an oil droplet on the mesh under water. In water, an oil/water/solid composite interface formed after water was absorbed into the polymer network. The IPN hydrogel-coated mesh exhibited underwater superoleophobicity with an oil contact angle of $153.92 \pm 1.08^\circ$ while the one of semi-IPN hydrogel coating is $141.50 \pm 0.50^\circ$ (the contact angle of oil droplet under water on bare stainless steel mesh is 117.75°). Because of the introduction of hydrophilic groups in the hydrogels, the coated mesh showed improved wettability compared with the bare mesh. Also the roughness of the coating played an important role on the wettability. As a result, an obvious increase was observed in contact angle after crosslinking of GA with PVA due to a coarser surface. It was already reported that the bigger the oil contact angle, the higher intrusion pressure of oil.¹⁶ So it can be expected that the IPN hydrogel coating would endure high intrusion pressure.

To test the stability of the hydrogel coating, the contact angle was measured after immersing the hydrogel-coated mesh in water for several days. In Figure 3, a stable contact angle was observed for the IPN hydrogel-coating even after immersing in water for 10 days. However, for the semi-IPN hydrogel coating, there was an increase of contact angle after one-day immersion, then the change of contact angle became negligible. The difference can be attributed to the different hydrogel structure. For the IPN hydrogel, the polymer interchains were constrained due to high crosslinking density. As a result, the structure was more stable. In contrast, PVA chains were free in the semi-IPN hydrogel and might cause a change in interface property before the conformational stability was reached.

To evaluate the role of IPN on the mechanical strength of the coating, the semi-IPN bulk hydrogel was first prepared following the same procedure as the hydrogel coating without the stainless steel mesh. Then the hydrogel was immersed in the GA solution (0.2 wt %, 5 days) to obtain an IPN bulk hydrogel. The result showed that mechanical property of the hydrogel

coating was also improved by introducing IPN structure into the hydrogel (Figure 4 left). The semi-IPN hydrogel broke up at a stress of 45.79 ± 11.92 kPa, while the IPN hydrogel at a stress of 97.00 ± 7.69 kPa in high water content (water contents of two hydrogels were 99.5% and 99.0% accordingly). The mechanical stress of the IPN hydrogel was about two times of that sustained by the semi-IPN hydrogel. Besides, it was clearly observed that the IPN hydrogel coating showed a better abrasion resistance than the semi-IPN one (Figure 4 right). So we can infer that the IPN hydrogel coated mesh can endure higher intrusion pressure and abrasion endurance during separation. It was worthy to note that the mechanical strength and wettability of the coating can be easily adjusted by varying the amount of GA since the GA had an important impact on the network size and surface roughness.

Separation of Oil-Water Mixture

Oil-water separation experiment was performed on the IPN hydrogel-coated mesh. Various oils and organic solvents including diesel, gasoline, hexane and petroleum ether were used. As shown in Figure 5, the oil-water mixtures and organic solvent-water mixtures (oil to mixture is 30 v/v%) have been successfully separated and no visible oil was observed in the separated water. The separation efficiency of IPN hydrogel coated mesh for the four mixtures was above 99.8% while the one of semi-IPN was lower in each case (Figure 5). By introducing mechanically strong IPN hydrogel coating on the stainless steel mesh, the coated mesh can selectively separate oil from water with the advantages of high separation efficiency and stable wettability. This work provided a facile and versatile way to fabricate oil-water separation materials.

CONCLUSIONS

In this work, we developed a simple process to fabricate mechanically strong IPN hydrogel-coated mesh for oil-water separation. In the coating process, crosslinking reaction between PVA and GA produced the second network which interpenetrated into the first network PAA crosslinked by BIS. This caused the shrink of the semi-IPN hydrogel network and

provided a coarse surface. Besides, the IPN hydrogel was proven to be mechanically strong and abrasion resistant. The IPN hydrogel-coated mesh exhibited a high oil-water separation efficiency of above 99.8%. This work provided a facile and versatile way to fabricate oil-water separation materials.

ACKNOWLEDGMENTS

This work was supported by the National Natural Science Foundation of China (51163015) and the Program for New Century Excellent Talents in University (NCET-11-1072).

REFERENCES

1. Wang, S.; Li, M.; Lu, Q. *ACS Appl. Mater. Interfaces* **2010**, *2*, 677.
2. Shi, Z.; Zhang, W.; Zhang, F.; Liu, X.; Wang, D.; Jin, J.; Jiang, L. *Adv. Mater.* **2013**, *25*, 2422.
3. Feng, L.; Zhang, Z.; Mai, Z.; Ma, Y.; Liu, B.; Jiang, L.; Zhu, D. *Angew. Chem. Int. Ed.* **2004**, *43*, 2012.
4. Zhang, L.; Zhang, Z.; Wang, P. *NPG Asia Mater.* **2012**, *4*, e8.
5. Zhu, Q.; Pan, Q.; Liu, F. *J. Phys. Chem. C* **2011**, *115*, 17464.
6. Hayase, K. K. G.; Fukuchi, M.; Kaji, H.; Nakanishi, K. *Angew. Chem. Int. Ed.* **2013**, *52*, 1986.
7. Ono, T.; Sugimoto, T.; Shinkai, S.; Sada, K. *Nat. Mater.* **2007**, *6*, 429.
8. Xu, L. P.; Zhao, J.; Su, B.; Liu, X.; Peng, J.; Liu, Y.; Liu, H.; Yang, G.; Jiang, L.; Wen, Y. *Adv. Mater.* **2013**, *25*, 606.
9. Kulawardana, E. U.; Neckers, D. C. *J. Polym. Sci., Part A: Polym. Chem.* **2010**, *48*, 55.
10. Ju, H.; McCloskey, B. D.; Sagle, A. C.; Wu, Y.-H.; Kusuma, V. A.; Freeman, B. D. *J. Membr. Sci.* **2008**, *307*, 260.
11. Sun, T.; Feng, L.; Gao, X.; Jiang, L. *Acc. Chem. Res.* **2005**, *38*, 644.
12. Yao, X.; Song, Y.; Jiang, L. *Adv. Mater.* **2011**, *23*, 719.
13. Liu, M.; Wang, S.; Wei, Z.; Song, Y.; Jiang, L. *Adv. Mater.* **2009**, *21*, 665.
14. Jung, Y. C.; Bhushan, B. *Langmuir* **2009**, *25*, 14165.
15. Jin, M.; Li, S.; Wang, J.; Xue, Z.; Liao, M.; Wang, S. *Chem. Commun.* **2012**, *48*, 11745.
16. Xue, Z.; Wang, S.; Lin, L.; Chen, L.; Liu, M.; Feng, L.; Jiang, L. *Adv. Mater.* **2011**, *23*, 4270.
17. Yang, J.; Zhang, Z.; Xu, X.; Zhu, X.; Men, X.; Zhou, X. *J. Mater. Chem.* **2012**, *22*, 2834.
18. Zhang, F.; Zhang, W. B.; Shi, Z.; Wang, D.; Jin, J.; Jiang, L. *Adv. Mater.* **2013**, *25*, 4192.
19. Wen, Q.; Di, J.; Jiang, L.; Yu, J.; Xu, R. *Chem. Sci.* **2013**, *4*, 591.
20. Cao, Y.; Liu, N.; Fu, C.; Li, K.; Tao, L.; Feng, L.; Wei, Y. *ACS Appl. Mater. Interfaces* **2014**, *6*, 2026.
21. Zhou, X.; Zhang, Z.; Xu, X.; Guo, F.; Zhu, X.; Men, X.; Ge, B. *ACS Appl. Mater. Interfaces* **2013**, *5*, 7208.
22. Lee, W. F.; Chen, Y. J. *J. Appl. Polym. Sci.* **2001**, *82*, 2487.
23. Podsiadlo, P.; Kaushik, A. K.; Arruda, E. M.; Waas, A. M.; Shim, B. S.; Xu, J.; Nandivada, H.; Pumphlin, B. G.; Lahann, J.; Ramamoorthy, A. *Science* **2007**, *318*, 80.